

An Improved Feed Forward PWM Control for MPPT of Solar PV Systems Under Varying Atmospheric Conditions

P.Sathya*[‡], R.Natarajan**

*Department of Electronics Engineering, VIT University, Vellore, Tamil Nadu- 632 014, India.

**Department of Mechanical Engineering, VIT University, Vellore, Tamil Nadu- 632 014, India.

(p.sathya@vit.ac.in, natarajan@vit.ac.in)

[‡]P.Sathya; Second Author, VIT University, Vellore, Tel: +91 979 090 2453,

Fax: +91 416 224 3092, p.sathya@vit.ac.in

Received: 05.10.2015 Accepted:17.11.2015

Abstract- The objective of this paper is to harvest maximum power from the solar panel using voltage based MPPT circuit for low power application under varying atmospheric conditions. A voltage based tracking system consisting of a voltage sensor, DC-DC boost converter, maximum power point tracker and a LED lighting load is designed and developed. The analog MPPT controller using direct feed forward PWM control signal for DC-DC converter operated in the continuous conduction mode is the principle block performing the tracking operation. Since the output of solar panel is nonlinear, the optimal power point will vary due to change in irradiance and temperature. Irrespective of the change in atmospheric conditions, the voltage sensor developed here has the ability to generate accurate reference voltage in accordance with the panel output and thereby maintains maximum power at the load. The experimental results have proved a power conversion efficiency of 97.48 % in clear sky condition, and (92.64 to 95.48) % in partial shading conditions resulting from the feed forward control technique employed in the MPPT circuit. The proposed tracking system is less complex and low cost one that has high tracking efficiency with less fluctuation in real time dynamic conditions compared to that of conventional tracking algorithms.

Keywords Boost converter, Feed forward, MPPT, Pulse width modulation (PWM), Power conversion efficiency.

1. Introduction

Solar photovoltaic is a renewable power source that directly converts the irradiance into electrical power without complexity. The power generated from the panel depends on many factors such as intensity of irradiance, temperature, angle of incidence and so on. Due to the variation of these parameters the operating point at which maximum power generated in the panel also varies. In order to track the optimum point at varying conditions, it is necessary to use a maximum power point tracker (MPPT). For a stand alone PV system using DC loads, the MPPT is formed by a converter of any topology and a control circuit using a MPP seeking algorithm. This seeking algorithm can be classified as quasi seeking (indirect control), true seeking (direct control) and

artificial intelligence controls. The quasi seeking type consists of curve fitting, look up table, open circuit voltage and short circuit current methods. In the past many researches have been performed on these algorithms for use in MPPT. Initially the curve fitting method of indirect control employing mathematical modelling of solar cell with one diode / two diode/ advanced model was used, but it faced difficulty in realizing analog/digital control. Next, the look up table method was used that required a large memory capacity for storing values corresponding to different climatic conditions faced resource difficulty. Then the open circuit voltage and short circuit current methods of indirect control are involved in tracking. They have assumed a linear variation between the open circuit voltage (short circuit current) and maximum voltage (maximum current) and are

interrupted frequently at every instant of change in irradiation to measure the parameters. This results in power loss and also the maxima obtained by this method is not an accurate one at all varying conditions. To avoid the frequent interruption in the above system, a pilot cell is added along with the existing panel for measuring the open circuit voltage [1, 2]. This method also results in an approximate MPP during sudden change in climatic conditions.

The direct control or true seeking approach involves the Perturb and Observe (P&O), incremental conductance and feedback methods. The P&O algorithm is based on an iterative method of perturbing the operating point and observing its change in the output power. This is the most commonly used algorithm in tracking, but it is not capable of tracking the optimum point under rapidly changing atmospheric conditions and also it fluctuates around the MPP at steady state [3]. The incremental conductance algorithm is also similar to that of P& O algorithm that has an ability to track the MPP under sudden change in climatic conditions and also no oscillations at steady state. The major drawback associated with this system is that the control circuit is too complex and tracking is slow. To improve the efficiency and enhance fast convergence, a variable step size is employed in the incremental conductance method [4]. The artificial intelligent controllers employing fuzzy logic and neural networks have gained great attention in the recent years and are trying to betterment the tracking. Very few neural network based MPPT are successful in tracking the maximum point under varying atmospheric conditions, but those are all complex in nature [5-7]. The simple and fast methods to track the MPP are the constant voltage and constant current based methods that are implemented for low and high power applications [8-11]. In these methods, a constant climatic condition is assumed and a linear relation is developed between the optimum point parameters and open circuit voltage/ short circuit current of solar panel. Hence the MPP achieved by these methods are close to optimum point and are lagging in locating the MPP exactly at all climatic conditions.

All the conventional MPPT methods are employed for tracking in clear sky conditions, but they are not suitable for dynamically changing atmospheric conditions. In the current trend, PV power generation is installed in many commercial and residential buildings that suffers mainly from the shading problem. Providing solution for the shading problem under dynamically fast changing climatic conditions with high tracking efficiency is the requirement now that drives many researchers towards it. In the recent years, a Particle swarm optimization algorithm for partial shading conditions is designed and simulated that showed a tracking efficiency of 99% [12]. The draw back of the system is that it is too complex and is apt mostly for high power applications. Similarly, a Sinusoidal extremum method of MPPT with 98% [13] and a Voltage Window Search (VWS) method of MPPT with 97.97% [14] are developed for tracking optimum point under partial shading conditions. In addition, a global MPPT controller using voltage band based method employing bypass diodes is designed and simulated that showed a significant improvement in tracking [15]. In addition, even numerical model based methods are also

developed to improve the tracking under shading conditions [16].

The analytical comparison of MPPT methods have shown that most efficient tracking methods are complex in nature and its implementation becomes difficult in real time. So a simple and cost effective MPPT suitable for varying climatic conditions has to be developed. From the literature it is found that voltage based feed forward method is less complex, and also its implementation is feasible and reliable. But the drawback is its accuracy of tracking is close to the optimum point rather than locating actual point. The objective of this paper is to design and develop a simple and cost effective voltage based MPPT circuit for low power applications that will locate the optimum point at varying atmospheric conditions with high accuracy.

2. Design Methodology of feed forward PWM control Technique

The block diagram presenting the technique of the feed forward control is shown in fig. 1. It consists of a Solar panel, DC/DC boost converter, maximum power point tracker (MPPT) and a lighting load. A thin film solar panel (0.395m x 1.25 m) with an area of 0.493 m² made up of poly crystalline solar cells is used in this project as an energy source. The current – voltage characteristics of this panel is tested initially before connecting it to the load and the results obtained from the test is discussed in the results section.

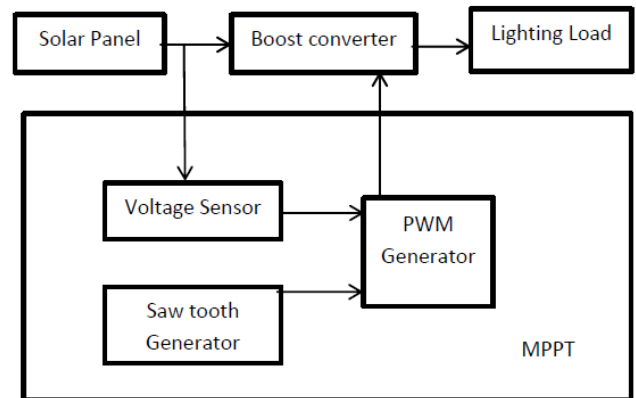


Fig.1. Block diagram of Feed forward PWM control technique

2.1. Design of DC-DC Boost Converter

A DC-DC boost converter is used to convert dc voltage at the input to a different dc voltage at the output. The circuit diagram of the boost converter is shown in fig.2. It consists of a MOSFET switch controlled by PWM signal. When the MOSFET is switched on, the inductor starts storing energy from the panel until T_{ON} period. Meanwhile, the reverse biased diode isolates the output from the circuit and capacitor supplies the load current. When the MOSFET is switched off, the inductor starts discharging and the current flows through the diode, and capacitor to load. The discharged voltage and instant panel voltage together contributes for the output voltage, hence it is always higher than the input voltage. The ON and OFF of the switch is controlled by the

PWM signal. A boost converter with varying input of (6-22)V to give regulated output of 30V dc is designed. The equations followed for the design of boost converter depicted in equations (1-7) is referred from [17].

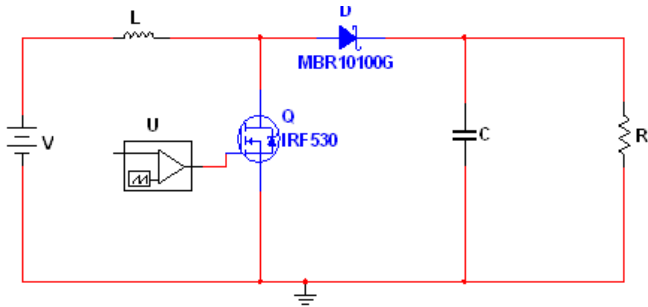


Fig. 2. Circuit diagram of DC-DC Boost converter

Assuming the inductor current rises linearly from I_1 to I_2 during T_{ON}

$$V_i = L \frac{\Delta I}{t_1} \tag{1}$$

And inductor current falls linearly from I_2 to I_1 in time t_2

$$V_i - V_o = -L \frac{\Delta I}{t_2} \tag{2}$$

Where $\Delta I = I_2 - I_1$, is the ripple current of inductor

$$\Delta I = \frac{V_i t_1}{L} = \frac{(V_i - V_o) t_2}{L} \tag{3}$$

Substituting $t_1 = DT$ and $t_2 = (1 - D)T$, the average output voltage is

$$V_o = \frac{V_i T}{t_2} = \frac{V_i}{1 - D} \tag{4}$$

This gives duty cycle as

$$D = 1 - \frac{V_i}{V_o} \tag{5}$$

The minimum value of inductance and switching frequency for continuous current in the boost converter is therefore

$$L_{min} = \frac{D(1 - D)^2 R}{2f} \tag{6}$$

The capacitor value for the circuit is determined by the equation is

$$C = \frac{D}{R(\Delta V_o / V_o) f} \tag{7}$$

2.2 Design of LED Lighting load

A lighting load is designed using high brightness white LEDs having a forward voltage of 3.2V and forward current of 60mA. It is arranged in 8x8 array form as shown in fig.3, in which each row has 8 LED connected in series that draws

total current of 480 mA from the source. This wizard require 75Ω resistors with atleast ½ watts (500 mW). Each resistor dissipates 270 mW contributing a power loss of 2.16 watts in the resistors and the LED dissipates 12.29 W. Hence the total power dissipated in the LED array lighting load is 14.45 W. The effective impedance of the lighting load is 62 Ω.

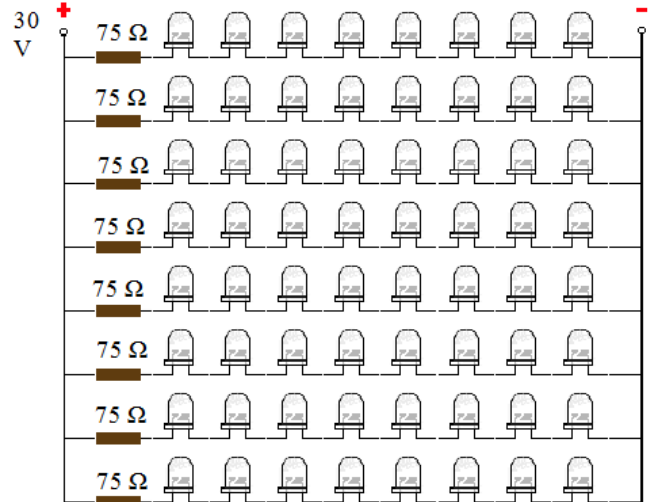


Fig. 3 Design of LED Lighting Load

2.3 Numerical values of the Practical design

The design specifications to meet the desired output: $V_{in} = (6 - 22)V$, $V_{out} = 30V$, $V_m=15V$ and $R_L= 62\Omega$.

The duty cycle for the peak power transfer at standard test condition (STC) is determined using equation (5) as 50%.

$$D = 1 - \frac{15}{30} = 0.5$$

The minimum inductance value for the desired output is obtained from equation (6) as follows.

$$L_{min} = \frac{0.5(1 - 0.5)^2 62}{2 \times 20000} = 194 \mu H$$

The practical value of the inductor should be more than the actual value to compensate the power loss. Hence a value of 200μH is chosen for the practical purpose. A cylindrical type inductor is designed and implemented in the circuit. The design equation followed for making practical inductor is given in equation (8).

$$L = \frac{d^2 n^2}{l + 0.45d} \tag{8}$$

Where,

- L = Inductance in μH
- n = Number of turns = 180 turns
- d = Diameter of winding = 2.4 cm
- l = Length of winding = 8.2 cm

$$L = \frac{(2.4cm)^2 180^2}{8.2cm + (0.45 \times 2.4)} = 201.10 \mu H$$

The capacitance value is determined using equation (7) with a ripple factor of 0.0125.

$$C = \frac{0.5}{62 \times 0.0125 \times 20000} = 32.26 \mu F$$

The standard capacitor value close to 32.26μF is 47μF which is used in the hardware implementation.

2.4 Maximum Power Point Tracking(MPPT)

Solar cell has a point at which the voltage and current results in a maximum power referred as maximum power point (MPP). For a DC operated load, this point specifically varies with respect to changes in solar insolation, load impedance and temperature. It is always advisable to deliver the maximum power to the load, irrespective of changes in climatic conditions. Hence a MPPT circuit is used here that improves the energy harvesting in the proposed system.

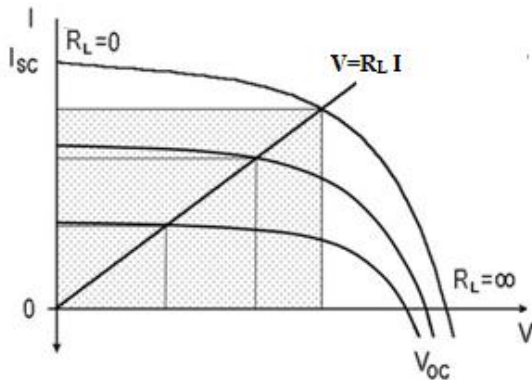


Fig. 4. Current-Voltage characteristics of PV panel at different work conditions.

A general I-V curve of a PV panel under different work conditions is shown in fig.4. Every point on the curve represents a power, but only one point will have the maximum power for a specific condition. For a given resistive load, the load line ($V=I R_L$) will intersect the panel characteristic curve at any point that may be near or far from the MPP. If the load impedance is not matched with the impedance of the panel at MPP, then only a fraction of the power at MPP will be transferred to the load resulting in power loss. In order to transfer the maximum power from the source to the load, impedance matching has to be done. This is done by the MPPT circuit that finds the source impedance at each instant of solar insolation and matches with the load requirement. According to Maximum Power Transfer theorem, the power output of a circuit is maximum when the impedance of the circuit (source impedance) matches with the load impedance. The load impedance is matched with the source impedance using the relation as shown in equation 9.

$$R_{eq} = (1 - D)^2 R_L \tag{9}$$

Where,

$$R_L = \frac{V_{out}}{I_{out}} \tag{10}$$

The duty cycle required to obtain maximum power is shown in equation (11).

$$D = 1 - \sqrt{\frac{R_{eq}}{R_L}} \tag{11}$$

2.4.1 Voltage Sensor

The MPPT circuit consists of a voltage sensor for generating reference voltage, sawtooth wave generator and a comparator for producing PWM signal. The voltage sensor is a potential divider network that generates the reference voltage as per the equation (12).

$$V_{ref} = V_{in} \frac{R_2}{R_1 + R_2} \tag{12}$$

It is designed based on the input and output voltage ranges of the converter. Here V_{in} varies from 6V to 24V and V_{out} has to be maintained at 30V. The voltage transfer function for the boost converter in continuous conduction mode (CCM) is given by

$$A_{dc} = \frac{V_{out}}{V_{in}} \tag{13}$$

The relation connecting duty cycle and transfer function is

$$D = 1 - \frac{\eta}{A_{dc}} \tag{14}$$

Considering a 90% converter efficiency, using equation (14), the minimum, nominal and maximum duty cycle values are found as $D_{min} = 0.28$, $D_{norm} = 0.58$ and $D_{max} = 0.84$ respectively. The maximum reference voltage that can be generated depends on the minimum duty cycle value and amplitude of saw tooth voltage (V_{ST}) as shown in equation (15).

$$V_{ref(max)} = (1 - D_{min}) V_{ST} \tag{15}$$

The $V_{ref(max)}$ obtained for this case is 7.2V. Now, the values of R_1 and R_2 belongs to voltage sensor can be found out using the following relation.

$$V_{ref(max)} = V_{in(max)} \frac{R_2}{R_1 + R_2} \tag{16}$$

Values of $R_1 = 2.2k\Omega$ and $R_2 = 1k\Omega$.

2.4.2 Saw tooth wave generator

A saw tooth waveform generator is designed using the timer circuit to produce a waveform of 10V peak and 20 kHz frequency as shown in fig.5. The function of the circuit is described as follows. The transistor, zener diode, resistors and capacitor forms a constant current source to charge the capacitor. Assuming the capacitor is discharged initially having zero voltage drop across it. The internal comparators of timer connected to pin 2 causes the timer output to go high

and it makes the capacitor to charge towards supply voltage. On charging, when the voltage across capacitor increases above $(2/3)^{rd}$ the supply voltage, the timer output goes low and shorts the capacitor to ground, thus discharging it. Again the output goes high when the voltage across capacitor decreases below $(1/3)^{rd}$ the supply voltage. This charging and discharging action of capacitor creates the saw tooth waveform. The frequency of the saw tooth waveform generated is given by equation (17) and is referred from [18].

$$f = \frac{V_{cc} - 2.7}{RCV_{pp}} \tag{17}$$

2.4.3 PWM generator

The PWM generator is designed using a comparator that produces an output pulse by comparing the inputs available at its input terminals as shown in fig.5. The reference voltage from the voltage sensor and the saw tooth waveform from the timer circuit are applied to the inverting and non –inverting terminals of the comparator respectively. At every instant, the reference voltage is compared with the amplitude of the saw tooth signal to generate a PWM signal.

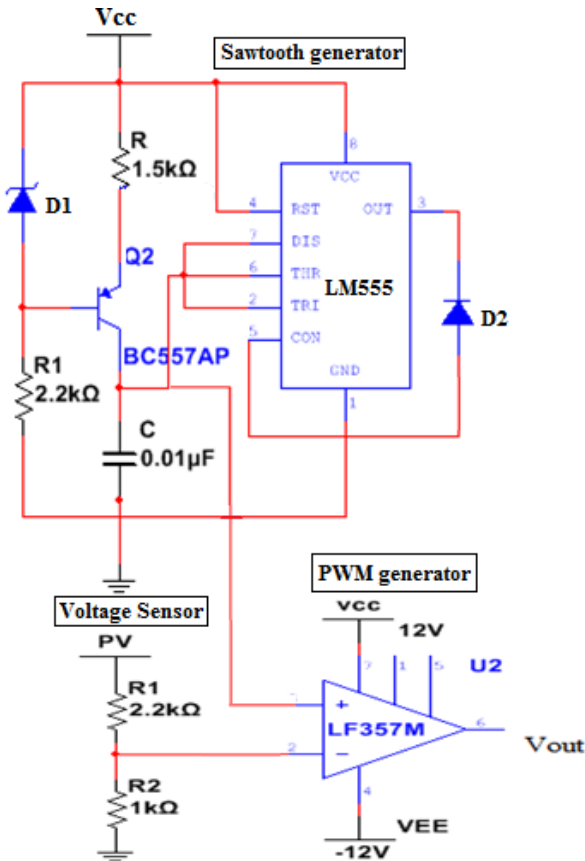


Fig. 5. Circuit diagram depicting the internal parts of MPPT

2.5 Principle of working

The solar panel generates the electrical power from the solar irradiation. Using the voltage sensor in contact with the panel output terminals, a reference voltage is generated at

each instant of input. When the irradiation or temperature changes, the voltage sensor will sense the panel output voltage and generates a corresponding reference voltage. This reference voltage is compared with the amplitude of saw tooth waveform for producing PWM signal. If the reference is greater than the saw tooth signal, PWM generator outputs high (ON), whereas for lower reference voltage, the output is low (OFF). This PWM signal acts as a gate control voltage for the MOSFET switch. The boost converter receives the input from panel, control signal from PWM generator and produces a regulated output. The MPPT circuit determines the source resistance resulting maximum power and accordingly adjusts the load resistance by changing the duty cycle of PWM signal. This in turn changes the conduction period of MOSFET and thereby resulting in regulated maximum output power.

3 Experimentation and Result analysis

3.1 Characteristic test of Solar Panel

The Solar panel is placed on an open terrace facing southwards tilted at a latitude angle of 12.93 degrees (Vellore) from the horizontal ground surface. Initially, the performance characteristic of the solar panel is determined at standard test conditions (STC: S = 1000 W/m², T= 25°C) to derive the electrical characteristics of the panel. From the observed results, the I-V curve and P-V curve are plotted and is shown in fig.6 and 7 respectively. The specifications of the solar panel used in the project is listed in table 1.

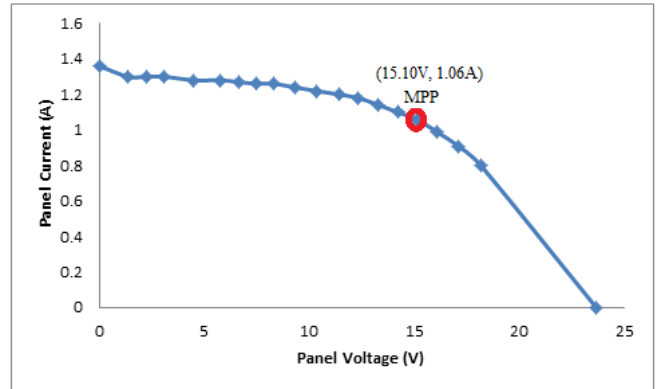


Fig. 6. Current-voltage characteristics of Solar panel at STC

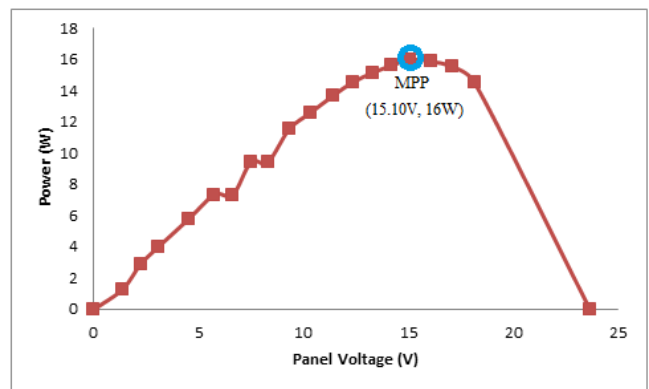


Fig. 7. Power-voltage characteristics of Solar panel at STC

3.2 Circuit Simulation

The complete circuit consisting of Solar panel, boost converter, MPPT and LED lighting load is designed in MULTISIM software version 13. The input voltage (PV) is varied from 6V to 22V and the corresponding output voltage, output current, control voltage and duty cycle are measured. From the measured values input power, output power and efficiency are calculated as shown in table 2. Then the MPPT section is removed from the system and simulation is performed again. The power tracking efficiency of the system with and without the MPPT section is compared and plotted in graph as shown in fig.8. The system with MPPT control resulted in an average efficiency of 96% whereas the system without MPPT section resulted around 45%. By using control circuit, it is possible to harvest maximum peak power from the source with minimal loss. Here, the loss of around 4% is reported that is due the power loss in the MOSFET switch, schottky diode and inductor. Finally the variation of duty cycle for different range of input obtained in simulation and experimentation is shown in fig.9. The distinct feature of this feed forward technique compared to conventional technique is that, it is not disconnected frequently to measure V_{OC} . The voltage sensor is designed to produce output equal to optimum value without depending on V_{OC} measurement.

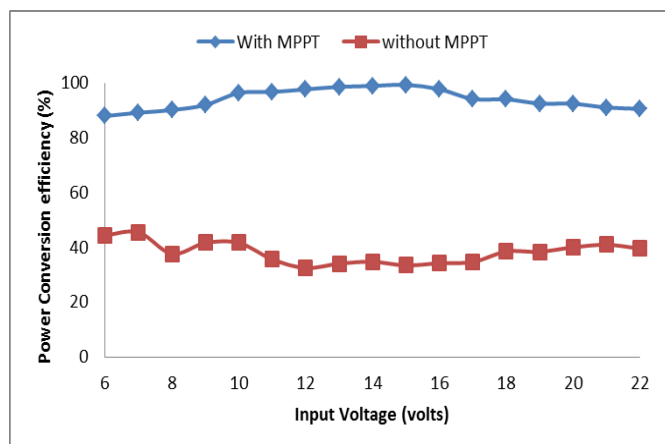


Fig. 8. Power conversion efficiency of the system with and without MPPT circuit

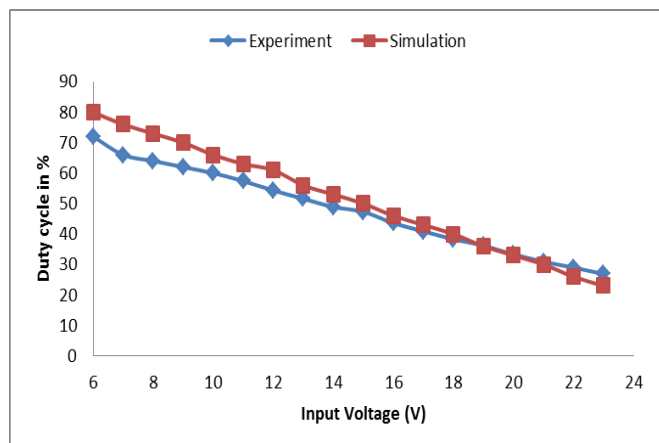


Fig. 9. Comparison of duty cycle variation in software simulation and hardware experimentation.

Table 2. Simulation results of the Feed forward PWM control MPPT system

V_{in} (V)	V_{out} (V)	V_c (V)	P_{in} (W)	P_{out} (W)	η (%)
6	25.80	1.875	11.88	10.45	87.96
7	26.12	2.205	12.04	10.74	89.20
8	26.42	2.500	12.48	11.25	90.14
9	26.76	2.813	12.42	11.43	92.03
10	27.10	3.146	12.20	11.76	96.39
11	27.22	3.437	12.32	11.92	96.75
12	28.13	3.750	12.72	12.43	97.72
13	28.85	4.062	13.13	12.95	98.63
14	29.35	4.375	13.44	13.30	98.96
15	29.74	4.687	14.25	14.16	99.34
16	29.46	5.010	13.92	13.61	97.77
17	29.39	5.312	13.60	12.81	94.19
18	29.32	5.625	13.50	12.70	94.07
19	29.31	5.937	13.68	12.66	92.54
20	28.62	6.250	13.40	12.39	92.46
21	28.46	6.572	13.02	11.86	91.09
22	27.92	6.884	12.76	11.56	90.60

3.3 Hardware Implementation

The complete experimental set up consisting of Solar panel, boost converter, MPPT and lighting load are connected together as shown in fig.10. For the boost converter, an IRF530 Power MOSFET, MBR10100G schottky diode, an inductor of 200 μ H and a capacitor of 47 μ F are recommended for hardware implementation. For the comparator circuit, LF357 op-amp comparator with 50V/ μ s slew rate is used. A 555 timer along with zener diode and BC557 is used for saw tooth wave generation. The functionality of the system is tested initially in the laboratory by applying a variable power supply in the input side and the corresponding output parameters are measured and verified for its accuracy. Then, the MPPT circuit using feed forward control technique is integrated with the solar output to determine its tracking ability under varying atmospheric conditions. The setup is continuously monitored under solar insolation right from 7.00 am in the morning to 5.00 pm in the evening on different days to assure its performance. Specifically the observations done on a day under clear sky and partial cloudy conditions (25% shading and 50% shading) are presented here. For partial cloudy condition, the panel is shaded manually by 25% and 50%, and then the observations are recorded. The electrical parameters like

input voltage, input current, output voltage, output current and temperatures are measured at an interval of 1 hour from 7 am to 5 pm on the day of experimentation for all three conditions.

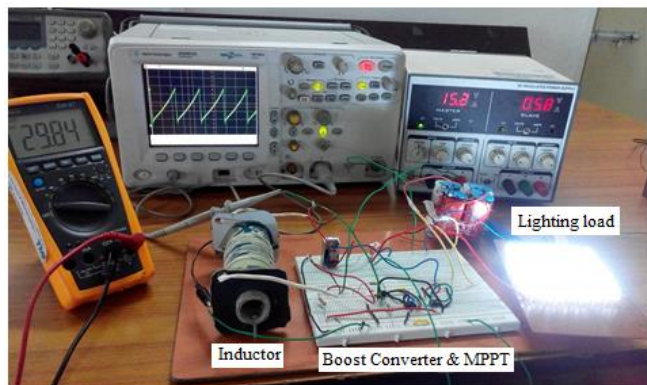


Fig. 10. Experimental set up displaying the hardware circuit and results

3.3.1 Case (i) Clear Sky condition

In clear sky condition, the entire panel receives the solar irradiation and all the cells are contributing for the net current. The variation in the solar insolation and ambient temperature resulting in varied input voltage and current contributing for the input power and the corresponding output parameters are shown in table 3.

Table 3. Simulation results of the Clear sky condition

Time (hours)	V _{in} (V)	I _{in} (A)	V _{out} (V)	I _{out} (A)	η (%)
7	22.4	0.38	29.72	0.27	94.27
8	23.2	0.35	29.88	0.26	95.67
9	22.6	0.48	29.92	0.36	99.29
10	22.1	0.53	30.00	0.38	97.33
11	21.2	0.58	30.03	0.40	97.69
12	20.7	0.6	30.02	0.40	96.68
13	20.2	0.62	30.03	0.41	98.31
14	19.3	0.63	30.02	0.40	98.76
15	20.3	0.54	30.00	0.36	98.52
16	22.4	0.44	29.98	0.32	97.34
17	22.8	0.36	29.91	0.27	98.39
Average					97.48

Under clear sky condition, it is observed that variation in input voltage is from 20.2V to 23.2V, current varying from 0.35 A to 0.63A, resulting in input power variation in the range of 8.12W to 12.52W due to varying solar insolation and temperature. The corresponding output parameter is also varied in accordance with variation in input parameters. The

output voltage is varied from 29.72.1V to 30.03V, current is varied from 0.26A to 0.41A resulting in output power range of 8.02W to 12.31W. The overall power conversion efficiency is varied from 94.27 to 98.76% resulting in an average value of 97.48%. The input and output power observed from the hardware experimentation is plotted in fig.11.

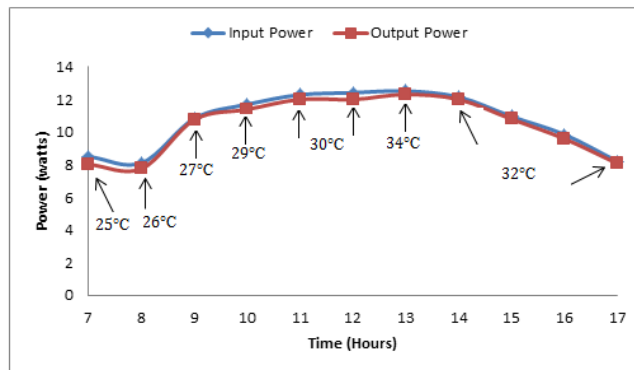


Fig. 11. Input and output power observed in clear sky condition.

3.3.2 Case (ii) Partial Shading condition (25%)

Table 4. Simulation results of the Partial shading condition (25%)

Time (hours)	V _{in} (V)	I _{in} (A)	V _{out} (V)	I _{out} (A)	η (%)
7	21.2	0.37	29.6	0.24	90.57
8	22.3	0.39	29.9	0.28	96.26
9	22.6	0.43	30.01	0.31	95.73
10	22.5	0.43	30.02	0.31	96.18
11	22.7	0.44	30.01	0.32	96.15
12	22.7	0.44	30.01	0.32	96.15
13	22.0	0.42	29.9	0.30	97.08
14	22.0	0.41	29.8	0.29	95.81
15	21.7	0.46	29.7	0.32	95.21
16	21.3	0.33	29.6	0.23	96.86
17	21.2	0.33	30.0	0.23	94.34
Average					95.49

To establish 25% partial shading condition, one-fourth of the panel is covered with opaque material and is done to assess the performance of the panel under partial cloudy conditions. This step is executed immediately after completing the clear sky measurement. Again the variation in input and output parameters due to varying solar insolation and temperature are recorded. From the measured values, power conversion efficiencies are calculated. It showed a variation of 21.2V to 22.7V, 0.33A to 0.46 A at the input side resulting in an input power of 6.996W to 9.988W.

Output parameters varied in respect to the input are 29.6V to 30.02V, 0.24A to 0.32A resulting in an output power of 6.6W to 9.60W. The range of power conversion efficiencies obtained at this partial shading condition is from 90.57% to 97.08% resulting in an average efficiency of 95.49%. The observed values are tabulated in table 4. The input and output power observed in 25% partial shading condition is plotted in fig.12.

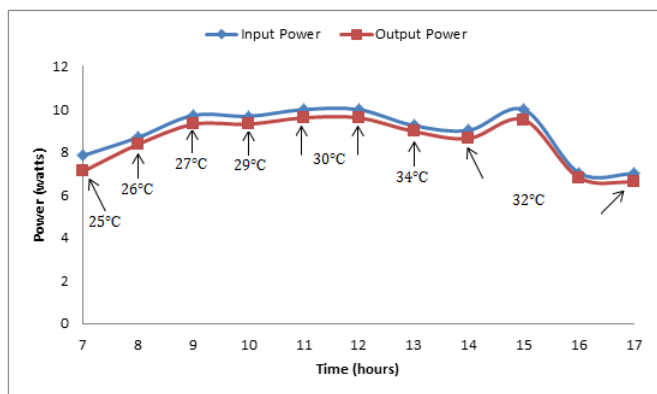


Fig. 12. Input and output power observed in 25%- partial shading condition

3.3.3 Case (iii) Partial Shading condition (50%)

The ability of the tracking system to harvest maximum power under 50% shading of the panel is considered as it could be the worst case of shading. To establish this condition, half of the panel is covered with opaque material so that it will not receive any incoming solar radiation in the covered section. The capacity of maximum energy generation of the exposed remaining half is tested in the same way as that of the previous method. This test is carried out instantly after completing the clear sky and 25% partial shading condition in the same duration. Measured values with respect to time due to variation in solar insolation and temperature are tabulated in table 5. The range of variation in electrical parameters are 20.1V to 21.7V in voltage, 0.32A to 0.5A in current, and 6.727W to 10.05W in power at the input side, whereas at the output side, 29.4V to 30.01V in voltage, 0.21A to 0.31A in current, and 6.237W to 9.145W in power. This resulted in a power conversion efficiency ranging from 84.88% to 93.9% with an average value of 92.64%. The input and output powers obtained from 50% partial shading condition is shown in fig.13.

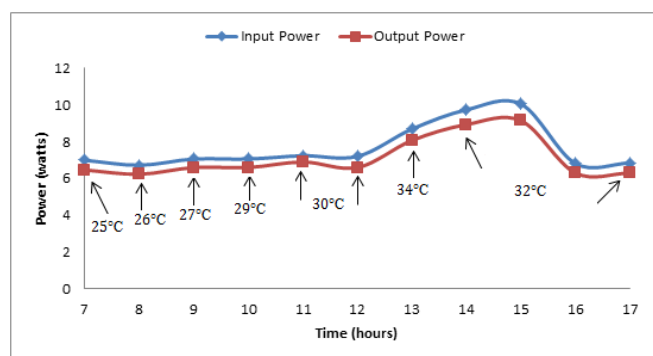


Fig. 13. Input and output power observed in 50%- partial shading condition

Table 5. Simulation results of the Partial shading condition (50%)

Time (hours)	V _{in} (V)	I _{in} (A)	V _{out} (V)	I _{out} (A)	η (%)
7	21.2	0.33	29.4	0.22	92.45
8	21.7	0.31	29.7	0.21	92.72
9	21.4	0.33	30.01	0.22	93.49
10	21.4	0.33	30.01	0.22	93.49
11	21.3	0.34	30.0	0.23	95.28
12	21.2	0.34	30.0	0.22	91.56
13	20.7	0.42	29.9	0.27	92.86
14	20.3	0.48	29.8	0.30	91.75
15	20.1	0.50	29.5	0.31	90.99
16	21.3	0.32	30.0	0.21	92.43
17	21.4	0.32	30.01	0.21	92.03
Average					92.64

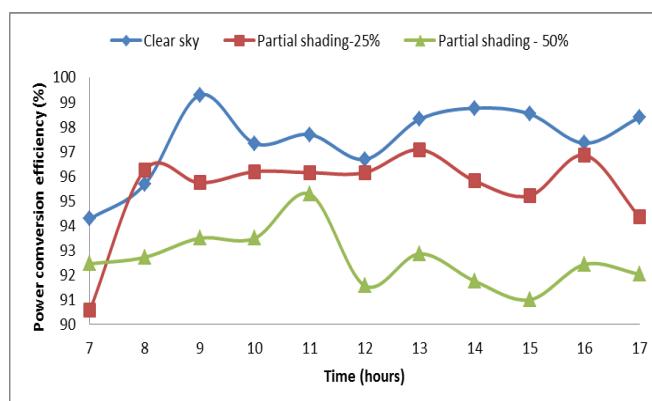


Fig. 14. Comparison of efficiency in all three cases

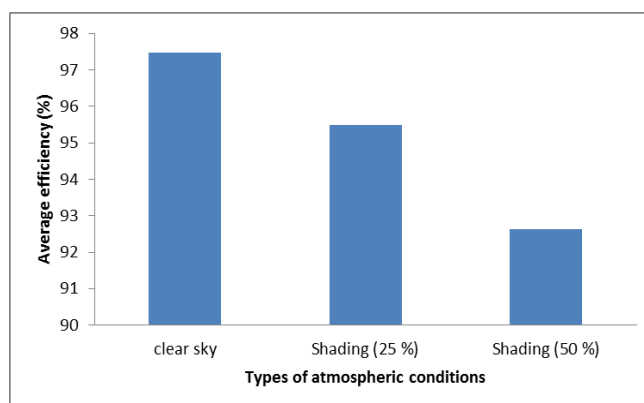


Fig. 15. Comparison of average efficiency in all three cases

The effect of irradiation and temperature on power conversion efficiency of the PV system in all three cases is shown in fig.14 and 15 respectively. This clearly proves that in clear sky condition, the designed system is extracting maximum power and its average conversion efficiency is 97.48%. The remaining 2.52% is due to the power loss in the MOSFET switch and other passive components. Even under the worst case partial shading condition also, this system has the ability to extract maximum power and is evident from the fact that average conversion efficiency is well above 92%. This accounts for a considerable amount of improvement in tracking due to the effective design of analog controller compared to the earlier ones. This feed forward system has produced improved performance compared to earlier feed forward technique due to accurate computation of control value resulting from voltage sensor and is independent of V_{OC} measurement. In earlier feedback techniques, The system is interrupted inbetween tracking for measurement of V_{OC} that led to power loss which is eliminated in the improved system. Moreover a constant reference voltage is compared with solar output values that resulted in approximate optimum point in the earlier feed forward method, whereas here control voltage corresponding to instant solar irradiation and temperature is involved in tracking optimum power point. The results obtained from this proposed system is validated by comparing its efficiency with other algorithms reported so far in table 6.

Table 6. Comparison of feed forward technique results with other popular techniques.

MPPT techniques	Tracking efficiency (%)
Perturb & Observe [3]	92
Incremental Conductance [4]	92.3
Sinusoidal Extremum Seeking [13]	98
Voltage Window Search [14]	97.97
Particle Swarm Optimization [12]	99.5 (Simulation)
Constant Voltage method [11]	95
Voltage feed forward PWM control	97.48

4 Conclusion

In this paper, an efficient voltage based feed forward analog PWM controller operated in continuous conduction mode has been proposed and developed for MPPT of Solar PV systems. The developed controller is integrated with solar panel for tracking the MPP under varying atmospheric conditions. The simulation and experimental results have proved that the system has the capability to track the MPP and also to regulate the output at sudden change in climatic conditions. It showed tracking efficiency greater than 97 % in clear sky condition, around 95% in medium shading and greater than 92% in worst case partial shading conditions. The experimental results are validated by comparing the efficiency of the proposed system with popular efficient

tracking techniques. This comparative result has showed that this method is has the capability to harvest maximum power even under worst case shading condition. The advantages of the system are simple, less complex and low cost, so that it can be used for almost all stand- alone low power applications.

References

- [1] B. Subudhi, and R. Pradhan, “A Comparative Study on Maximum Power Point Tracking Techniques for Photovoltaic Power Systems”, IEEE Transactions on Sustainable Energy, vol. 4, no.1, pp. 89-98, January 2013.
- [2] R. A. Reza, M. M. Hassan, S. Jamsab , “ Classification and comparison of maximum power point tracking techniques for photovoltaic system: a review”, Renew. Sustain. Energy Rev., vol.19, pp. 433-443, 2013.
- [3] T. Tafticht, K. Agbossou, M.L. Dombia, A. Cheriti, “An improved maximum power point tracking method for photovoltaic systems”, Renew. Energy, vol.33, pp.1508-1516, 2008.
- [4] F. Liu, S. Duan, F. Liu, B. Liu, Y. Kang, “A variable step size INC MPPT method for PV systems”, IEEE Trans. Indus. Electron. Vol.55, no.7, pp. 2622-2628, 2008
- [5] B. N. Alajmi , K. H. Ahmed , S. J. Finney, and B.W. Williams, “Fuzzy logic control approach of a modified hill –climbing method for maximum power point in micro-grid standalone photovoltaic system”, IEEE Trans. Power Electron, vol.26, no.4, pp.1022-1030, 2011
- [6] M. R. Vincheh , A. Kargar, G. A. Markadeh, “A Hybrid Control Method for maximum power point tracking (MPPT) for Photovoltaic Systems”, Arab. J. SCi. Eng., vol.39, pp. 4715-4725, 2014.
- [7] M.A. Abido, M. Sheraz Khalid, M.Y. Worku, “An efficient ANFIS based PI controller for Maximum power point tracking of PV systems”, Arab. J. SCi. Eng., Vol.40, pp.2641-2651, 2015.
- [8] J. Ahmad, and H. J. Kim, “ A Voltage Based Maximum Power point Tracker for Low Power and Low cost Photovoltaic Applications”, World Academy of Science, Engineering and Technology, vol. 60, pp. 712-715, 2009
- [9] O. L. Laperia, M.T. Penella, M. Gasulla, “ A new MPPT method for low power solar energy harvesting”, IEEE Trans. Ind. Electron., vol.57, no.9, pp.3129-3138, 2010
- [10] P. Sathya, R. Natarajan, S. Kothari, “Analog Maximum power point tracker using constant reference voltage technique”. Int. J. Applied Eng. Research, vol.8, no.14, pp.1677-1684, 2013
- [11] P. Sathya, and R. Natarajan, , “Design and Implementation of 12V/24V Closed loop Boost Converter for Solar powered LED Lighting System”. Int. J. Eng. & Technology, vol.5, no.1, pp.254-264, March 2013.
- [12] K. Ishaque, Z. Salam, A. Shamsudin and M. Amjad, “ A direct control based maximum power point tracking

- method for photovoltaic system under partial shading conditions using particle Swarm optimization algorithm”, *Applied Energy*, vol.99, pp. 414-422, June 2012
- [13] R. Leyva, C. Olalla, H. Zazo, C. Cabal, A. Cid-Pastor, I. Queinnec, and C. Alonso, “MPPT Based on Sinusoidal Extremum- Seeking control in PV Generation”, *International Journal of Photoenergy*, vol.12, pp.1155-1162, 2012
- [14] M. Boztepe, F. Guinjoan, G. Velasco- Quesada, S. Silvestre, A. Chouder, and E. Karatepe, “ Global MPPT scheme for Photovoltaic string Inverters based on Restricted Voltage Window Search Algorithm”, *IEEE Transactions on Industrial Electronics*, vol. 61, no.7, pp. 3302-3312, July 2014.
- [15] N. Gokmen, E. Karatepe, F. Ugranli, and S. Silvestre, “Voltage band based global MPPT controller for photovoltaic systems”, *Solar Energy*, vol. 98, pp. 322-334, November 2013.
- [16] L. Cristaldi, M. Faifer, M. Rossi, and S. Toscani, “ An Improved Model- Based Maximum Power Point Tracker for Photovoltaic Panels”, *IEEE Transactions on Instrumentation and Measurement*, vol. 63, no.1, pp. 63-71, January 2014.
- [17] M. H. Rashid, *Power Electronics: Circuits, Devices and Applications*, 3rd edition, 11th impression, Pearson education, pp. 190-194, 2012.
- [18] D. Roy Choudhury, *Linear Integrated Circuits*, 2nd edition, New Age International Publishers, ch.5 & 8, 2007.